ANL-7234

100
1/30/67

Fast Reactor

ANL-7234

Argonne National Laboratory

LABORATORY INVESTIGATIONS IN SUPPORT OF FLUID-BED FLUORIDE VOLATILITY PROCESSES

Part XII. The Melting-point Diagram for the System Uranium Hexafluoride-Plutonium Hexafluoride

by

L. E. Trevorrow, M. J. Steindler,
D. V. Steidl, and J. T. Savage

DISCLAIMER

LEGAL NOTICE

Printed in the United States of America
Available from
Clearinghouse for Federal Scientific and Technical Information
National Bureau of Standards, U. S. Department of Commerce
Springfield, Virginia 22151
Price: Printed Copy $3.00; Microfiche $0.65

ANL-7234
Chemical Separations Processes for Plutonium and Uranium (TID-4500)
AEC Research and Development Report

ARGONNE NATIONAL LABORATORY
9700 South Cass Avenue
Argonne, Illinois 60439

LABORATORY INVESTIGATIONS IN SUPPORT OF FLUID-BED FLUORIDE VOLATILITY PROCESSES

Part XII. The Melting-point Diagram for the System Uranium Hexafluoride-Plutonium Hexafluoride

by

L. E. Trevorrow, M. J. Steindler,
D. V. Steidl, and J. T. Savage

Chemical Engineering Division

July 1966

Operated by The University of Chicago
under
Contract W-31-109-eng-38
with the
U. S. Atomic Energy Commission

Other reports in this series are:

Part I — The Fluorination of Uranium Dioxide-Plutonium Dioxide Solid Solutions (ANL-6742).

Part II — The Properties of Plutonium Hexafluoride (ANL-6753).

Part III — Separation of Gaseous Mixtures of Uranium Hexafluoride and Plutonium Hexafluoride by Thermal Decomposition (ANL-6762).

Part IV — The Fluid-bed Fluorination of U_3O_8 (ANL-6763).

Part V — The Radiation Chemistry of Plutonium Hexafluoride (ANL-6812).

Part VI — A. The Absorption Spectrum of Plutonium Hexafluoride

B. Analysis of Mixtures of Plutonium Hexafluoride and Uranium Hexafluoride by Absorption Spectrometry (ANL-6817).

Part VII — The Decomposition of Gaseous Plutonium Hexafluoride by Alpha Radiation (ANL-7013).

Part VIII — Analysis of an Accidental Multigram Release of Plutonium Hexafluoride in a Glovebox (ANL-7068).

Part IX — The Fluid-bed Fluorination of Plutonium-containing Simulated Oxidic Nuclear Fuel in a $1\frac{1}{2}$-inch-diameter Reactor (ANL-7077).

Part X — A Literature Survey on the Properties of Tellurium, Its Oxygen and Fluorine Compounds (ANL-7142).

Part XI — Vapor-Liquid Equilibria in the System Uranium Hexafluoride-Plutonium Hexafluoride (ANL-7186).

TABLE OF CONTENTS

TABLE OF CONTENTS

LIST OF FIGURES

TABLE

LABORATORY INVESTIGATIONS IN SUPPORT OF FLUID-BED FLUORIDE VOLATILITY PROCESSES

PART XII. The Melting-point Diagram for the System Uranium Hexafluoride-Plutonium Hexafluoride

by

L. E. Trevorrow, M. J. Steindler,
D. V. Steidl, and J. T. Savage

ABSTRACT

Thermal analysis was used to determine melting points of UF_6-PuF_6 mixtures containing 0 to 100 m/o PuF_6. All mixtures melted at temperatures between the melting points of the pure components; neither maximum- nor minimum-melting mixtures were observed. The solid-liquid equilibria involve a continuous series of solid solutions, and the temperature-composition diagram exhibits the shape characteristic of such a series. Solidus points were observed at temperatures lower than those calculated for ideal behavior; this difference is attributed to fractional crystallization.

I. INTRODUCTION

The main objective of the fluoride volatility process is the recovery of both uranium and plutonium from spent nuclear fuel. In the process, fluorinating agents act on oxidized nuclear fuel to produce the hexafluorides of uranium and plutonium, which can be separated from each other and also from the fission-product fluorides because of differences in their physical and chemical properties.

Several unit operations considered in fluoride volatility processes involve mixtures of UF_6 and PuF_6 in the condensed states. This report describes experimental determinations of the melting points of UF_6-PuF_6 mixtures carried out to obtain information on phase equilibria in the condensed states.

II. EXPERIMENTAL DETAILS

A. Containment of Volatile Fluorides

All experimental work with UF_6-PuF_6 mixtures was performed in a metal manifold constructed of nickel tubing and fittings. The manifold incorporated Monel diaphragm valves* and a number of 1-in.-diam valves** with brass bodies, Monel bellows, and Teflon seats. The transfer of PuF_6 and UF_6 from one vessel to another in the manifold was carried out by vacuum distillation at room temperature.

A three-module, $2\frac{1}{2}$-tier CENHAM glovebox[1] ($3\frac{1}{2}$ x $8\frac{1}{2}$ x 10 ft) housed the manifold and all equipment for handling PuF_6. Figure 1 shows the glovebox and associated facilities. Laboratory air, used as the glovebox atmosphere, entered the box through two high-efficiency AEC filters (12 x 12 x 6 in.) arranged in parallel. The air flowed out of the box through four filters of the same type (two parallel sets of two filters in series) and into a 6-in.-diam aluminum ventilation duct. The ventilation

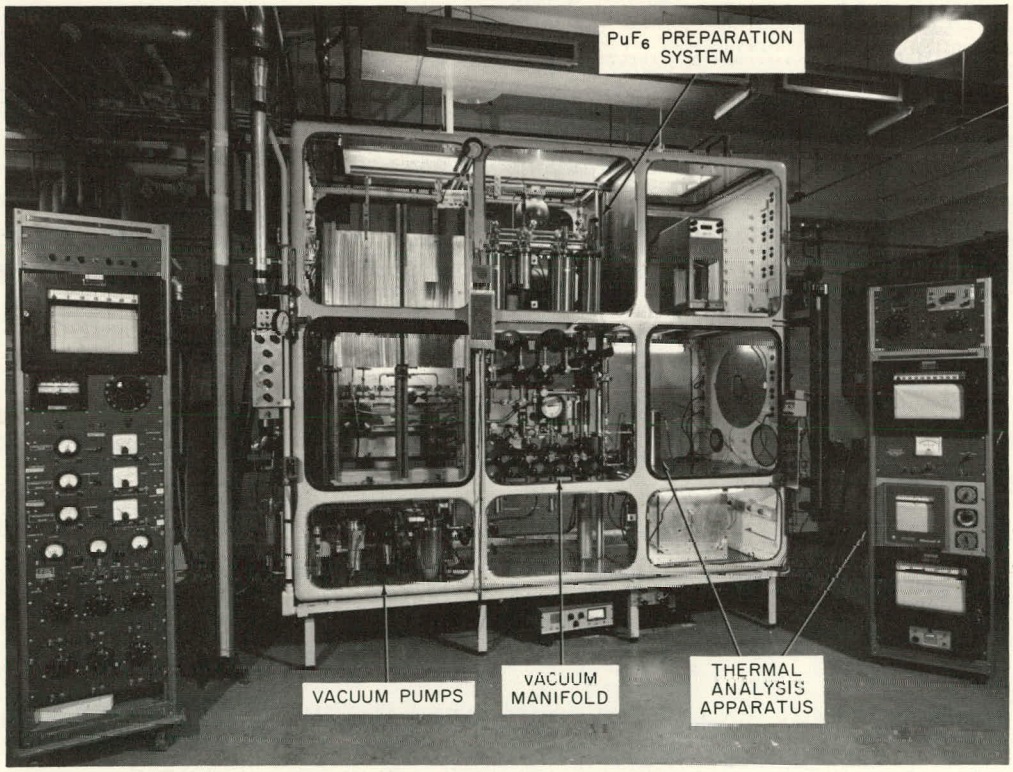

108-7534-B

Fig. 1. CENHAM Glovebox and Associated Apparatus Used in Thermal Analysis of UF_6-PuF_6 Mixtures

*Valves Nos. 411 and 413, Hoke Incorporated, One Tenakill Park, Cresskill, N. J.

**Vactronic Lab. Equipment, Inc., East Northport, Long Island, N. Y.

air then passed through an aqueous spray scrubber, and two AEC filters (24 x 24 x 12 in.) in parallel before discharge through a stack to the atmosphere.

B. Materials

1. Uranium Hexafluoride

The UF_6 used in this work was a portion of a larger batch originally obtained from Oak Ridge National Laboratory. Almost two-thirds of the original batch had been distilled away in previous experimental work, contributing to the purification of the UF_6 from low-boiling impurities (e.g., HF, CF_4, F_2). Emission-spectrographic analysis of the material indicated that the predominant impurities were phosphorus, at a concentration of <400 ppm, and As, B, Cs, Pd, Re, Sb, Sn, and Th at concentrations of <100 ppm. Two determinations of the triple point of a sample of the UF_6 yielded 64.1 and 64.2°C. The best literature value[2] for the triple point of UF_6 is 64.05°C.

2. Plutonium Hexafluoride

a. Preparation Apparatus. The PuF_6 was prepared in this laboratory by reaction of fluorine with PuF_4 at 550°C. Powdered PuF_4 was spread in a flat nickel boat (2 x 7 x 1/2 in.) within a Monel tube reactor ($2\frac{3}{8}$-in. diam) heated by a 1650-W cylindrical furnace.* A nickel diaphragm pump** circulated fluorine at 600 to 800 cc/min over the PuF_4. The secondary diaphragm of the pump was inside the glovebox; the primary diaphragm and gear box were underneath the glovebox. An oil† column transmitted pulses from the primary diaphragm through a copper tube to the secondary diaphragm. A thermal flowmeter[3] monitored the gas flow rate. The gas stream leaving the reactor passed through four nickel traps in series, the first two of which were cooled in a dry ice-trichloroethylene slush to condense PuF_6 from the gas stream. Figure 2 is a schematic

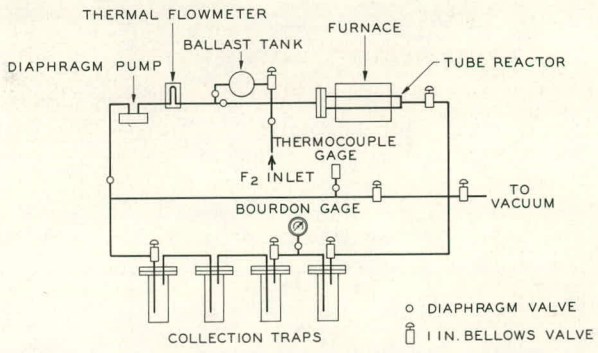

Fig. 2
Schematic Diagram of Apparatus Used to Prepare PuF_6

* Hevi-Duty Electric Co., Milwaukee, Wisconsin.

** Lapp Pulsafeeder No. CPS-1, Lapp Insulator Co., Inc., LeRoy, N. Y.

† Halocarbon Oil, Series 411 E, Halocarbon Products Corp., 82 Burlews Court, Hackensack, N. Y.

diagram of the preparation apparatus. The collection traps are shown in the upper part of Fig. 1; the furnace and the reactor tube are shown in Fig. 3.

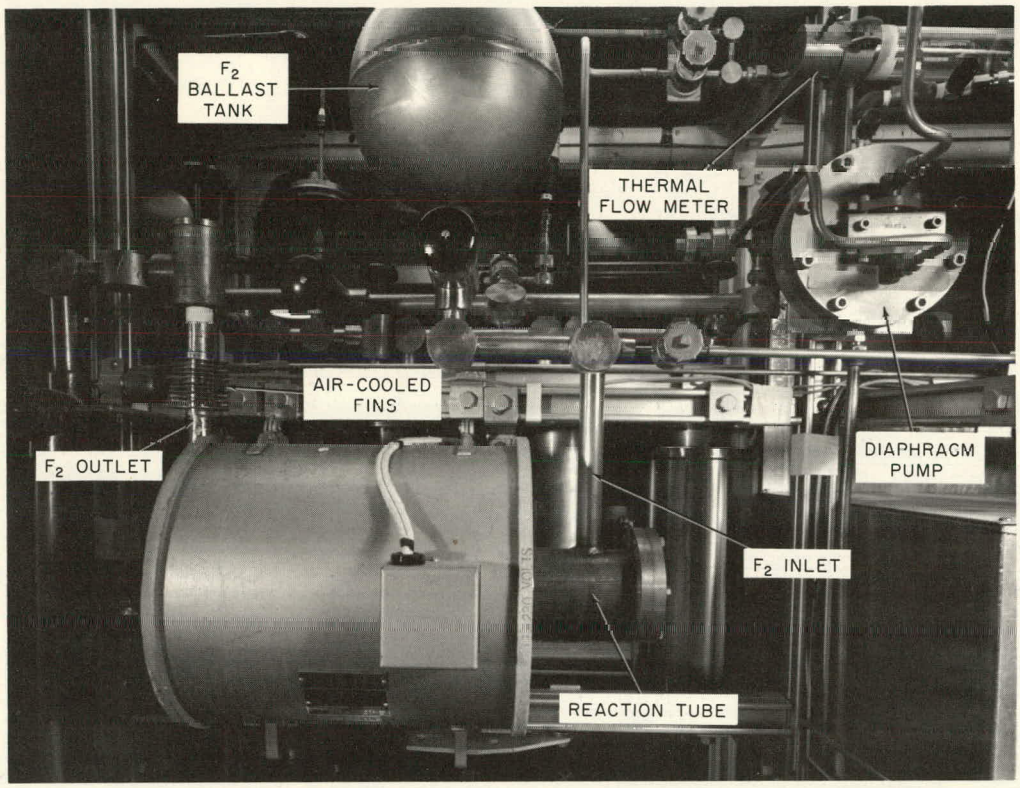

108-7531A

Fig. 3. Furnace and Tube Reactor Used to Prepare PuF_6

b. Typical Preparation Procedure. A typical preparation of a 60-g batch of PuF_6 was as follows: The reactor, containing the PuF_4, was evacuated to 0.01 to 0.02 Torr, and heated to 400°C. Heating and evacuation were continued for about 4 hr. The heating was usually carried out during an afternoon; then the furnace power was turned off, and the evacuation was continued while the furnace and reactor cooled slowly overnight. The following morning, the preparation apparatus was filled with fluorine (1 atm) at room temperature, gas circulation was started, and the furnace was heated to 550°C. A 60-g batch of PuF_6 was normally prepared in 10 to 14 hr.

c. Purification Procedure. After preparation, the PuF_6 was freed from low-boiling impurities by a trap-to-trap distillation similar to that described by Weinstock and Malm.[4]

d. Evidence of Purity. The high purity of the PuF_6 product was confirmed by measurement of the triple point and also by the results of an emission-spectrographic analysis of the PuF_4. Two determinations

of the triple point of a sample of purified PuF_6 yielded 51.5 and 51.3°C. The best literature value[2] for the triple point of pure PuF_6 is 51.59°C, obtained by extrapolation of vapor-pressure data. The PuF_4, from which the PuF_6 was prepared, contained calcium (<25 ppm), iron (<20 ppm), and antimony (<20 ppm) as predominant impurities.

C. Apparatus for Thermal Analysis

1. Sample Tubes

Mixtures to be examined by thermal analysis were contained in a sample tube constructed of 1/2-in.-diam nickel tubing with a 20-mil wall. The tube was $1\frac{3}{4}$ in. long with a bottom well extending 1/4 in. along its central axis. The temperature of a mixture was measured by an Inconel-sheathed thermocouple inserted within the bottom well. The sample tube was bolted through a Teflon-gasketed flange to a brass valve body. Closure of the valve body and containment of the fluoride samples were effected by a 1/2-in. bellows assembly* with a Teflon seat. In this assembly, silver solder joined the phosphor bronze bellows to the valve stem. The sample tube assembly could be attached to a vacuum manifold by means of a 3/8-in. male flare fitting soldered to the opening of the brass valve body. The volume of the sample tube was about 4 ml when the valve was closed. Figure 4 is a pictorial drawing of the sample tube and valve assembly.

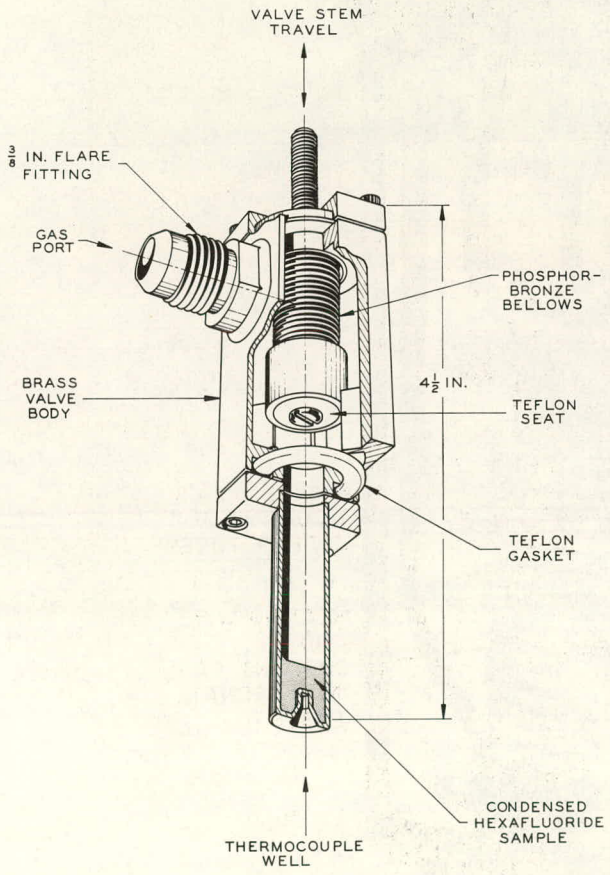

108-9845

Fig. 4. Sample Tube and Valve Assembly Used to Contain UF_6-PuF_6 Mixtures for Thermal Analysis

2. Sample-block Assembly

A mixture contained in the sample tube was subjected to thermal analysis while positioned in a cavity in a cylindrical nickel block, which was heated or cooled. The nickel block was wound with a double helix of 3/16-in.-OD copper tubing.

The nickel sample block was cooled by passing nitrogen, refrigerated to -60°C in a

*Veeco Vacuum Corp., 86 Denton Ave., New Hyde Park, Long Island, N. Y.

dry ice-trichloroethylene bath, through one copper helix. The block was heated by resistance-heating of an asbestos-covered Nichrome wire inserted in the second helix.

The nickel block was bolted to a flange, which hung on a tripod in a stainless-steel Dewar flask fitted with a Transite cover. A photograph of the tripod and nickel block with two sample tubes in place is shown in Fig. 5. Figure 6 is an exploded pictorial drawing of the entire assembly, hereafter termed the sample-block assembly. Figure 7 illustrates the placing of a sample tube into the sample-block assembly.

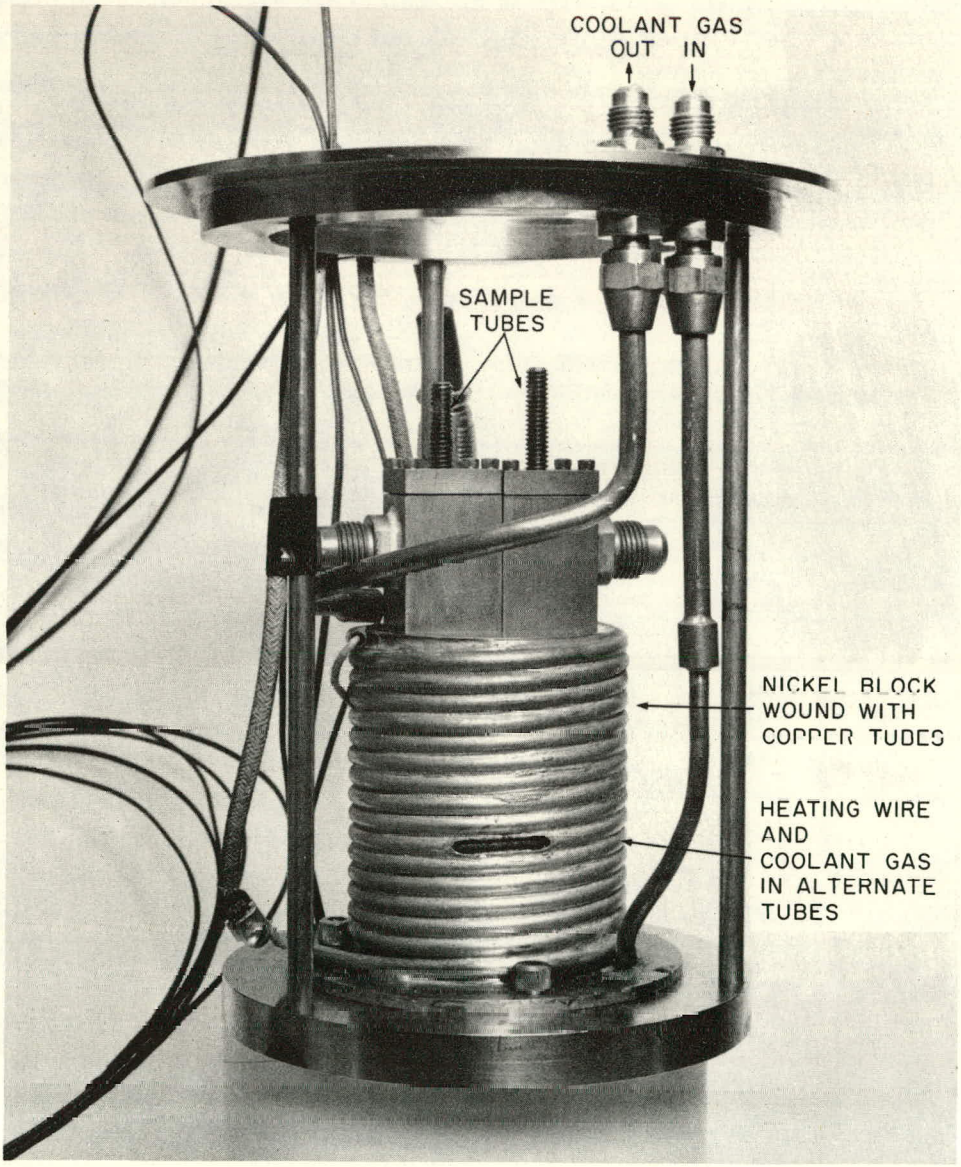

108-7537A

Fig. 5. Sample-block Assembly for Thermal Analysis

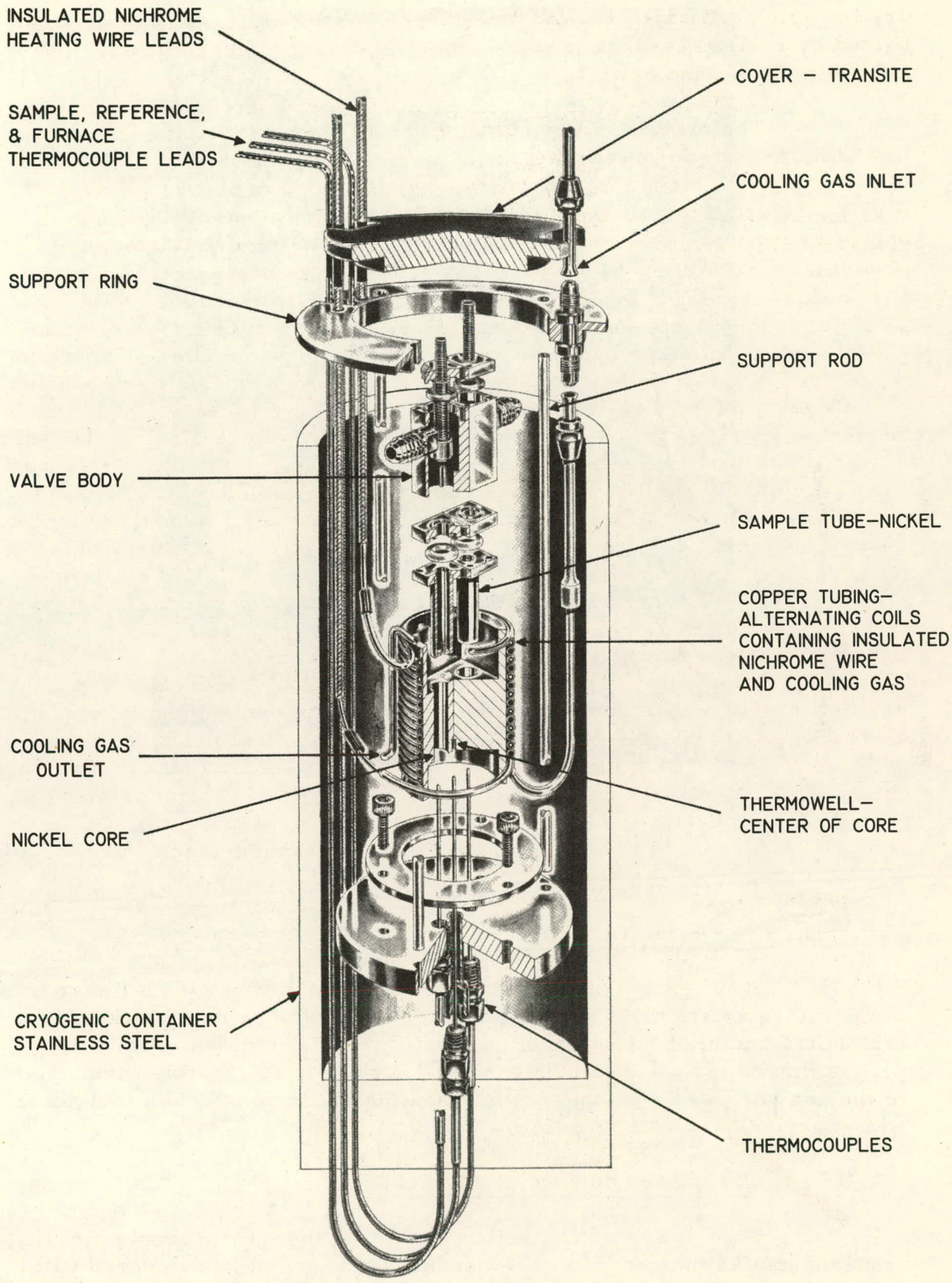

Fig. 6. Exploded View of Sample-block Assembly

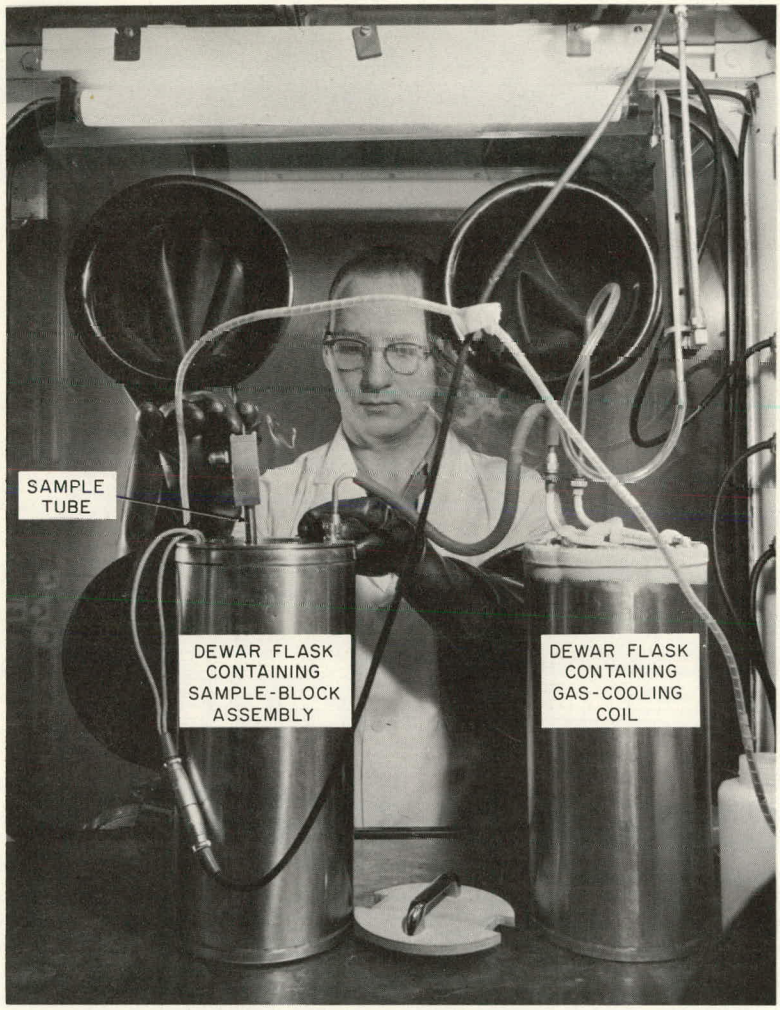

108-8428A

Fig. 7. Operation of Thermal-analysis Apparatus; Placing a Sample Tube into Sample-block Assembly

3. Temperature Control of Sample-block Assembly

A program controller* was employed to establish a linear time-temperature relationship for heating and cooling the sample block. A control unit** and a silicon-controlled rectifier, in conjunction with the programmer, provided proportioned, d.c. power to the heating wire. Most of the analyses were carried out at a heating rate of 0.3°C/min, but some were carried out at 0.6°C/min.

4. Thermocouple Circuit and Read-out

Figure 8 is a schematic diagram of the thermocouple circuit. Iron-constantan thermocouples, embedded in magnesia and covered with

* Minneapolis-Honeywell Regulator Co., Philadelphia, Pa., Electronik Strip Chart Proportioning Program Controller.

** Minneapolis-Honeywell, Electro-Volt Control Unit.

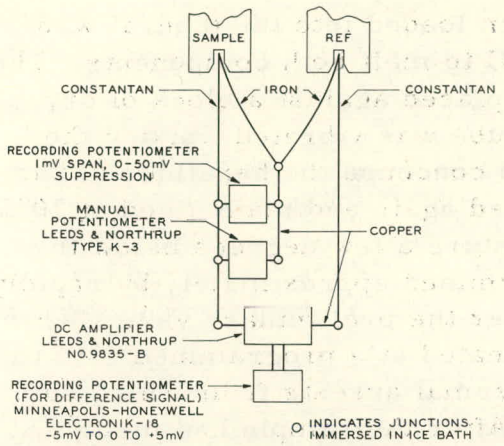

Fig. 8. Thermocouple Circuit for Thermal Analysis

Inconel sheaths, measured both the sample temperature and the difference in temperature between sample and reference tubes. The thermocouple wires were electrically insulated from the sheath. The signal of the thermocouple in the sample tube could be determined either by a recording potentiometer,* or by a manual potentiometer and a null meter.** The recording potentiometer was calibrated against the manual potentiometer before each experiment, and was also calibrated during an experiment whenever the zero suppression of the recording potentiometer was reset.

For differential thermal analysis, two tubes were positioned side by side in the nickel block. One tube contained the mixture to be examined by thermal analysis; the other tube, containing air, was a reference. Accurate readings for the differential thermocouple were obtained using air as the reference material. The voltage indicating the difference between the sample and reference thermocouples was amplified by an instrument† capable of multiplying the difference signal by factors varying from $2\frac{1}{2}$ to 100. The amplified signal was displayed by a strip-chart recorder†† with a zero center and a span of -5 to +5 mV.

D. Procedure for Thermal Analysis

Before an experiment, the sample tube was conditioned by evacuating the tube, filling it with fluorine gas at ~800 Torr, and then warming the tube with a heat gun. The fluorine was allowed to remain in the tube for 1 to 15 hr. The tube was then evacuated and weighed to obtain a tare.

A sample tube was loaded as follows: A sample of PuF_6 was measured by vaporizing it at 25°C into a ballast tank to an observed pressure. The PuF_6 sample was then condensed into the sample tube by cooling the bottom of the tube with liquid nitrogen or dry ice. The sample tube was removed from the vacuum manifold and weighed on a 1-kg-capacity automatic balance‡ to determine the weight of the PuF_6 sample. The sample tube was then reattached to the vacuum manifold, and a sample of UF_6 was measured and condensed into the sample tube in a similar manner. The sample tube was weighed again to determine the weight of the UF_6 sample.

*Minneapolis-Honeywell, Recording Potentiometer, 1-mV span, 0- to 50-mV suppression.

**Leeds and Northrup Co., Type K-3 Potentiometer; Null Meter Model No. 9834.

†Leeds and Northrup Co., Philadelphia, Pa., Model No. 9835-B.

††Minneapolis-Honeywell, Electronik 18 Recorder.

‡Mettler Instrument Corp., Princeton, N. J.

After both the PuF_6 and UF_6 had been loaded into the tube, it was placed in the nickel block and heated to 70°C to melt both components. The tube was then removed quickly, and the tip placed against a block of dry ice. When in contact with the dry ice, the tube was vibrated, mixing the components. This procedure also helped to condense the hexafluorides into the bottom of the tube. The tube was warmed again and maintained at 70°C for an hour; then it was cooled to a temperature a few degrees below the melting point. Thermal arrests were determined approximately by rapidly cooling or heating the sample mixture. After the preliminary values were obtained, the sample-block assembly was heated at a programmed rate to make more accurate observations of the thermal arrests from which solidus and liquidus temperatures were obtained. After the sample had melted, it was cooled, and the procedure was repeated for another determination of the melting point. Programmed thermal analysis was carried out two to five times on each mixture.

After the thermal analysis had been completed, the sample mixture was distilled into a waste trap filled with activated alumina. The sample tube was then detached from the brass valve assembly, and any solids were removed. If a mixture remained in a tube for several days between thermal analysis and emptying, a quantity of fluffy solid (presumably PuF_4 formed by radiation decomposition of PuF_6) accumulated in the tube. The sample tube was then reattached to the brass valve assembly, and the unit was placed on the vacuum line for reconditioning.

III. RESULTS

A. Interpretation of Thermal-analysis Curves

1. Heating Curves

Figure 9 shows examples of records of the voltages of both the sample thermocouple and the differential thermocouple obtained during the melting of a mixture of UF_6-PuF_6 (45.8 m/o UF_6). The shape of the record (melting curve) indicates that melting takes place over a temperature range. All mixtures yielded similar melting curves.

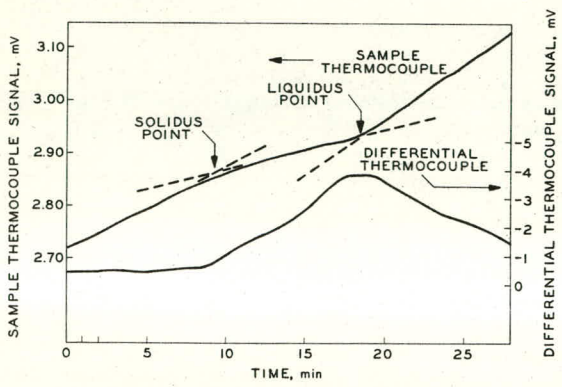

Fig. 9. Voltage Records of Thermocouples during Melting of a UF_6-PuF_6 Mixture (45.8 m/o UF_6)

In some cases, the breaks in the melting curves were less sharp than those illustrated by Fig. 9, particularly for the liquidus point. A round shoulder on a melting-point curve can be attributed to a thermal-absorption effect which is not large enough to

maintain the temperature difference between the sample and the sample-block assembly until the sample has completely melted. In such cases, the solidus and liquidus points were determined by intersections of the extensions of linear portions of the curves as indicated by Findlay.[5]

2. Cooling Curves

Because of supercooling effects, liquidus points could not be determined accurately from cooling curves. A typical mixture supercooled extensively and then crystallized suddenly. The heat-transfer characteristics of the sample-block assembly were such that the heat released in freezing was insufficient to raise the sample temperature enough to yield an accurate determination of the liquidus point from cooling curves even by an extrapolation procedure. A thermally-insulating sample tube or larger samples might have yielded accurate liquidus points by cooling curves. Bullard et al.,[6] using 1000 to 2500 g of UF_6 in freezing-point measurements, observed supercooling of only a fraction of a degree. Priest and Priest[7] controlled supercooling in UF_6 samples of 130 to 150 g by bumping the samples. Neither the use of manual bumping nor the use of an electric core-box vibrator eliminated the supercooling of the UF_6-PuF_6 samples, however. Small samples (1 to 4 g) were used in the present work to promote homogeneity in the absence of stirring.

The maximum temperature usually attained by the UF_6-PuF_6 mixtures upon crystallization after supercooling was the solidus point. The sharp maximum on the temperature record did not appear to be a reliable measure of the solidus point. Therefore, all data accepted as measures of the solidus and liquidus points were obtained from the records of melting determinations.

B. Solidus and Liquidus Temperatures

Voltages of the sample thermocouple corresponding to solidus and liquidus points were converted into temperatures using NBS Table No. 561.[8] Table I lists the solidus and liquidus temperatures in °C for the entire range of composition between 0 and 100 m/o UF_6. Since two to five melting

TABLE I. Temperatures of Thermal Arrests in UF_6-PuF_6 Mixtures

Mole Fraction[a] UF_6	Liquidus Point,[b] °C	Solidus Point,[b] °C	Correction of Mole Fraction UF_6 for Partial Vaporization[c]		Maximum Correction of Mole Fraction UF_6 for Radiation Decomposition[c]	Mole Fraction[a] UF_6	Liquidus Point,[b] °C	Solidus Point,[b] °C	Correction of Mole Fraction UF_6 for Partial Vaporization[c]		Maximum Correction of Mole Fraction UF_6 for Radiation Decomposition[c]
			At Liquidus	At Solidus					At Liquidus	At Solidus	
0.0506	53.0 ± 0.1	51.6 ± 0.1	-0.002	0.000		0.581	59.4 ± 0.9	57.1 ± 0.6	-0.002	-0.001	
0.132	53.6 ± 0.2	51.5 ± 0.4	-0.001	0.000	+0.002	0.677	60.3 ± 0.5	58.7 ± 0.4	-0.003	0.000	+0.005
0.141	53.6 ± 0.1	52.8 ± 0.1	-0.000	0.000		0.684	59.6 ± 0.1	58.3 ± 0.2	-0.003	-0.001	+0.005
0.220	54.0 ± 0.1	53.2 ± 0.2	-0.002	-0.001		0.714	60.9 ± 0.3	59.1 ± 0.2	-0.002	0.000	+0.004
0.244	54.2 ± 0.3	52.8 ± 0.1	-0.002	0.000	+0.004	0.751	60.9 ± 0.1	59.5 ± 0.3	-0.002	0.000	+0.004
0.307	55.6 ± 0.3	54.3 ± 0.0	-0.001	0.000		0.851	62.4 ± 0.3	61.3 ± 0.0	-0.001	-0.001	
0.323	54.7 ± 0.2	53.8 ± 0.1	-0.005	-0.001	+0.004	0.876	62.8 ± 0.1	61.8 ± 0.1	-0.001	-0.001	
0.388	57.0 ± 0.8	54.7 ± 0.3	-0.003	0.000	+0.005	0.924	63.6 ± 0.1	61.9 ± 0.1	-0.001	0.000	+0.001
0.458	56.9 ± 0.1	56.1 ± 0.2	-0.001	0.000		0.946	64.4 ± 0.4	62.5 ± 0.3	0.000	0.000	+0.001
0.501	57.8 ± 0.1	56.1 ± 0.2	-0.002	-0.001		0.964	64.0 ± 0.1	63.5 ± 0.0	0.000	0.000	
0.503	57.5 ± 0.4	55.8 ± 0.4	-0.004	-0.001							

[a]Mole fraction calculated from total weights of components.
[b]Listed values are averages of two to five determinations; the uncertainties are standard deviations of the averages.
[c]See Appendix A for details of calculation.

curves were obtained for each mixture, values for liquidus and solidus temperatures listed in Table I are averages, and the uncertainty values are standard deviations from the averages. The origins of the minor correction terms listed in Table I are discussed in Appendix A.

IV. DISCUSSION

A. Melting-point Diagram

All mixtures melted at temperatures between the melting points of the pure compounds. There was no evidence for the formation of any constant-melting mixtures (no maximum-melting mixture, no minimum-melting mixture). These observations and the shape of the melting curves indicated that solid-liquid equilibria in the UF_6-PuF_6 system involve a continuous series of solid solutions.

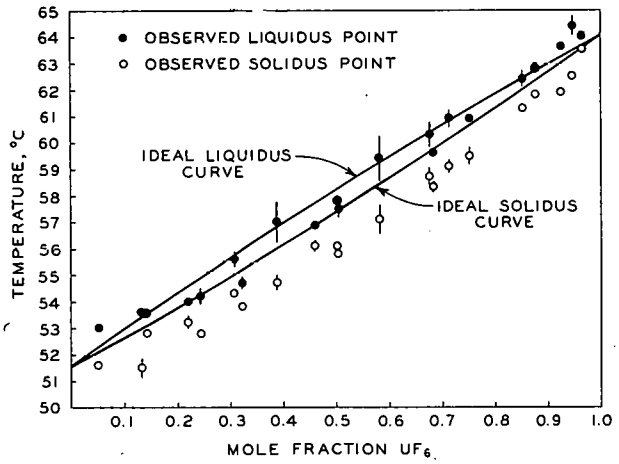

308-109

Fig. 10. Melting-point Diagram for the System UF_6-PuF_6

Figure 10, a plot of the solidus and liquidus temperatures against composition, shows the lens-shaped diagram characteristic of a continuous series of solid solutions. The stable phases in the various areas of the diagram are: only liquid above the lens, liquid in equilibrium with solid solution inside the lens, and only solid solution below the lens.

A mixture with a composition of 50.3 m/o UF_6 was cooled to -9°C in a search for any thermal arrests below the solidus point that would indicate a miscibility gap in the solid solution. No thermal arrests were observed between the solidus point and -9°C. The result of this cursory search, however, is not positive evidence that a miscibility gap is nonexistent. Even though the equilibrium state of a given solid system involves two phases, it may remain undetected by thermal analysis if the process of splitting into a two-phase system, involving diffusion in the solid state, is slow.[9]

B. Consideration of the Factors Influencing Solid Miscibility

A review of the physical properties of UF_6 and PuF_6, in the light of Hildebrand and Scott's discussion[10] of the influence of physical properties on solid miscibility, indicates that a high degree of solid miscibility in the UF_6-PuF_6 system is to be expected. Hildebrand and Scott discussed

three major influences on miscibility in the solid phase: heat of mixing, distortion energy, and crystal-structure compatibility.

1. Heat of Mixing

Mixtures exhibiting a large heat of mixing are apt to be incompletely miscible in the solid phase. According to regular solution theory, for two components with equal molal volumes, the partial molal energy of mixing of a component is[11]

$$\overline{\Delta E}_1^M = x_2^2 \left[(\Delta E^v)^{1/2} - (\Delta E^v)^{1/2}\right]^2, \quad (1)$$

where

$\overline{\Delta E}^M$ = energy of mixing = heat of mixing if volume change on mixing is negligible,[12]

ΔE^v = energy of vaporization = heat of vaporization - RT,

and

x_2 = mole fraction of component 2.

Measurements of the liquid densities of PuF_6 are not available; the only comparison of volumes of UF_6 and PuF_6 molecules is on the basis of calculations from X-ray diffraction data.[13] Since the crystals of UF_6 and PuF_6 are isomorphous,[13,14] the unit-cell volumes can be used as a comparison of their molal volumes. The small difference between the calculated unit-cell volumes for UF_6 (462.0 $\AA^3$) and for PuF_6 (461.4 $\AA^3$) indicates that the molal volumes can be considered equal for an estimate of the heat of mixing. Since the heats of vaporization of UF_6 and PuF_6 also differ only slightly (4588 cal/mole for UF_6, and 4456 cal/mole for PuF_6),[2] the heat of mixing calculated from Eq. 1 will be small.

2. Distortion Energy

A solid solution formed with a large distortion energy (lattice distortion caused by substituting molecules of a second component for the lattice molecules) will exhibit incomplete miscibility. Hildebrand and Scott[10] and Lawson[15] related the distortion energy to the square of the difference in molal volumes. As indicated above, the difference in molal volumes of UF_6 and PuF_6 is small; therefore the distortion energy should be small.

3. Compatibility of Crystal Structures

A system will exhibit incomplete miscibility in the solid phase if the crystal structures of the two pure components are incompatible. Since

the crystal structures of UF_6 and PuF_6 are isomorphous,[14] and since the sizes of the unit cells do not differ greatly,[13] there is no basis for the incompatibility of the crystal structures.

The expressions for heat of mixing and of distortion energy noted above are derived for spherical particles. It is assumed that these expressions can be applied to UF_6 and PuF_6 molecules, which approximate spherical geometry because of their octahedral symmetry,[16] nevertheless recognizing the evidence for the distortion of the UF_6 molecule in the solid state.[2,16-18]

Considering that the above three causes of incomplete miscibility in the solid phase are absent in the system UF_6-PuF_6, it is not surprising that the condensed-phase equilibria involve a continuous series of solid solutions.

C. Comparison of Observed Behavior with Ideal Behavior

The curves in Fig. 10, representing the locus of ideal solidus and liquidus temperatures, were calculated from the following equations developed by Seltz:[19]

$$N_1^{\ell} = \frac{1 - k_2\, e^{\Delta H_2/RT}}{k_1\, e^{\Delta H_1/RT} - k_2\, e^{\Delta H_2/RT}} \tag{2}$$

and

$$N_1^{S} = N_1^{\ell} k_1\, e^{\Delta H_1/RT}, \tag{3}$$

where

$$\left.\begin{aligned} k_1 &= \frac{1}{e^{\Delta H_1/RT_1}}, \\ k_2 &= \frac{1}{e^{\Delta H_2/RT_2}}, \end{aligned}\right\} \tag{4}$$

N_1^{ℓ} = mole fraction of component 1 in liquid phase,

N_1^{S} = mole fraction of component 1 in solid phase,

R = gas constant,

ΔH_1 = heat of fusion for component 1,

ΔH_2 = heat of fusion for component 2,

T = Kelvin temperature,

T_1 = melting point of component 1, °K,

and

T_2 = melting point of component 2, °K.

Simpler derivations of the same equations were outlined by Hildebrand and Scott[10] and also by Biswas and Bashforth.[20] The development of these equations is based on the assumption that Raoult's law holds for both the liquid solutions and for the solid solutions.

In an isoplethal comparison (at the same composition), all the observed solidus temperatures lie below the ideal values; the average deviation of observed solidus temperatures from the ideal curve is -1.0°C. In an isothermal comparison, the observed values are richer in UF_6 than the ideal system; the average deviation of observed solidus temperatures from the ideal values is +8.0 m/o.

The deviation of observed liquidus points from the ideal is somewhat less than the deviation of observed solidus points from the ideal. On an isoplethal basis, the average deviations of observed from ideal liquidus values are +0.3 -0.7°C. On an isothermal basis, the average deviations of observed from ideal liquidus values are +4.6 -2.1 m/o.

While the observed liquidus points are scattered in the vicinity of the ideal liquidus curve, the observed solidus points all lie below the ideal solidus curve. Three possible causes of the apparent bias of observed solidus points with respect to the ideal solidus curve are considered in Section D below.

D. Interpretation of Deviation of Observed Solidus Points from Ideal Behavior

1. Soluble Impurities

Soluble impurities can lower the solidus points of mixtures with little effect on the liquidus points.[21] This would be expected because at the liquidus point only small crystal nuclei should be in contact with the liquid phase, a situation more favorable to diffusion and the establishment of equilibrium than the situation at the solidus point where a relatively larger amount of solid is in contact with a small amount of liquid.

If an impurity were the cause of observed solidus points below the ideal solidus curve in the UF_6-PuF_6 system, the impurity most likely is HF, a product of the reaction of the hexafluorides with moisture. It is

suggested, however, that the presence of a soluble impurity is an unsatisfactory explanation because the impurity also would produce a lowering of the end points of the observed solidus curve, i.e., the melting points of the pure components; this behavior was not observed.

2. Fractional Crystallization

Fractional crystallization occurs if equilibrium is not established between the solid and liquid phases as a mixture cools.[22] If diffusion in the solid phase does not take place at a sufficient rate for the solid to remain uniform in composition and in equilibrium with the liquid, the first nucleus of solid is effectively removed from the equilibrium, and becomes the UF_6-rich core of a growing solid mass. The crystalline mass is pictured as a layered structure, each succeeding layer being poorer in the higher-melting component (UF_6). With the removal of UF_6-rich solid from the equilibrium, the composition of the remaining liquid becomes richer in the lower-melting component (PuF_6), and its freezing point continues to fall, approaching the freezing point of pure PuF_6 as the limit. As a result, if equilibrium is not established during freezing, the observed solidus temperature will be lower than the true value. Also, after complete crystallization, if diffusion has not proceeded far enough to homogenize the solid phase before a melting determination is performed, the outer layer of solid, rich in the lower-melting component, will be the first to melt; a solidus point that is lower than the true value will be observed. It is generally recommended[23] that a mixture be annealed at a temperature just below the solidus point before heating to determine the solidus point by a melting curve. To obtain observations of solidus points at equilibrium by thermal analysis or X-ray analysis, Wooley and Lees[24] found it necessary to anneal alloys at temperatures just below the solidus point for 2 weeks to 3 months.

Long annealing times were not considered for the system UF_6-PuF_6 because the effects of accumulation of relatively large amounts of PuF_4, formed by radiation decomposition of PuF_6, on both the composition and the temperature measurements, could not be clearly defined. The establishment of equilibrium between liquid and solid phases might have been promoted by an extremely low rate of cooling during freezing before the melting-point determination, but this technique was impossible because of the supercooling phenomenon; a typical mixture when cooled several degrees below the solidus point then appeared to freeze rapidly.

In one experiment, a completely crystallized mixture with a composition of about 50 m/o UF_6 was annealed for 1 hr at a few degrees below the observed solidus point. When the solid was remelted, the observed solidus point was unchanged. Thus, if the deviation of observed from ideal behavior is caused by fractionation, an annealing time of 1 hr is insufficient to remove the inhomogeneity.

3. Thermodynamic Expression of Deviation from Ideality

The deviation of observed solidus points from ideal solidus points in the UF_6-PuF_6 system could be treated in a manner analogous to treatments of similar systems, each expressing the deviations as activity coefficients or excess thermodynamic functions. Seltz[25] discussed the types of deviation from Raoult's law which determine the types of phase diagrams observed for binary systems with complete solid miscibility. Pitzer and Brewer[26] suggested that it is possible to assume ideal behavior in the liquid solutions and to calculate activity coefficients for the solid solutions. Scatchard and Hamer,[27] however, suggested that the calculation of isothermal-activity coefficients based on measurements in experiments at constant composition (as in thermal analysis), rather than at constant temperature, is not justified. Scatchard and Hamer recommended the use of analytical expression, involving only two parameters, for chemical potentials to construct solidus and liquidus curves to fit the observed points throughout the temperature range of the diagram. The two parameters can be related to excess free energies of mixing in the system.

However, considering that the PuF_6-UF_6 mixtures were not annealed for any appreciable periods, and lacking the assurance that the observed solidus points represent an equilibrium condition, the expression of the deviation from ideality in terms of activity coefficients or excess thermodynamic functions could be misleading, and therefore is not presented.

V. SUMMARY

The melting of UF_6-PuF_6 mixtures has been investigated using the techniques of thermal analysis. Mixtures with compositions covering the range from 0 to 100 m/o were prepared by distilling UF_6 and PuF_6 into nickel tubes. Compositions of the mixtures were calculated from direct weighings of the components.

Owing to the extensive supercooling of the mixtures, and, presumably, to the small sample sizes (1 to 4 g), the transition points could not be measured accurately from cooling curves. All solidus and liquidus points were therefore calculated from melting curves.

All melting phenomena occurred between the melting temperatures of the pure components, and each mixture melted over a temperature interval. These observations indicated that the solid-liquid equilibria involve a continuous series of solid solutions; the temperature-composition diagram has the lens shape characteristic of such a series.

Observed liquidus points scattered about the ideal liquidus curve, but all observed solidus points occurred at temperatures below the ideal

solidus curve. This behavior could be the result of soluble impurities, or a thermodynamic deviation from ideality, but it is quite likely the result of fractional crystallization during freezing preceding melting-point determinations, since the mixtures were not annealed in the solid state.

Two values of the triple point of pure PuF_6 were obtained by thermal analysis: 51.5 and 51.3°C. The best literature value[2] is 51.59°C, obtained from the intersection of vapor-pressure curves of solid and liquid phases.

APPENDIX A

Correction Terms

1. Corrections of Values of Mole Fraction

a. Correction for Vaporization

Because of vaporization and the difference in vapor pressures of UF_6 and PuF_6, the equilibrium composition of the mixture should differ from the initial composition determined by weighing the components. The volume of the closed sample tube was 4.9 ml. The calculated liquid volume of hexafluoride mixture was usually about 1 ml, and the remaining space was filled with a mixture of hexafluoride vapor. A corrected composition for both liquid and solid solutions was approximated using the following equation, based on the assumption that both the liquid and solid solutions follow Raoult's law:

$$N^{v}_{UF_6} = \frac{n_{UF_6} - p^{\circ}_{UF_6} X_{UF_6} \frac{V}{RT}}{\left(n_{UF_6} - p^{\circ}_{UF_6} X_{UF_6} \frac{V}{RT}\right)\left(n_{PuF_6} - p^{\circ}_{PuF_6} X_{PuF_6} \frac{V}{RT}\right)}, \qquad (5)$$

where

$N^{v}_{UF_6}$ = mole fraction of UF_6 corrected for vaporization,

X = mole fraction calculated from total amounts of UF_6 and PuF_6,

T = Kelvin temperature of solidus or liquidus point,

n = total moles of component,

V = volume of vapor space = $V_{total} - \frac{\text{total weight mixture}}{\text{density of condensed mixture}}$,

and

V_{total} = 4.9 ml.

For correction of mole fraction associated with liquidus temperatures:

$p^{\circ}_{UF_6}$ = vapor pressure (extrapolated) of supercooled UF_6 liquid;

$p^{\circ}_{PuF_6}$ = vapor pressure of PuF_6 liquid.

The density of the liquid mixtures was assumed to be a constant of 3.7 g/ml, obtained by extrapolation of the "pooled data" for the density of liquid UF_6 listed by Wertz and Hedge.[28]

For correction of mole fraction associated with solidus temperatures:

$p^{\circ}_{UF_6}$ = vapor pressure of pure UF_6 solid;

$p^{\circ}_{PuF_6}$ = extrapolated vapor pressure of pure PuF_6 solid.

The density of the solid mixture was assumed to be equal to that of pure UF_6 solid, 4.9 g/ml.[29]

The correction terms $(N^{v}_{UF_6} - X_{UF_6})$, which were added to the mole fraction $UF_6 (X_{UF_6})$ calculated from the total moles of UF_6 and PuF_6, are listed in Table I.

b. Correction for Radiation Decomposition

In the condensed state, pure PuF_6 is decomposed to PuF_4 by the alpha radiation from the various plutonium isotopes at a rate of about 2%/day.[30] In several cases, UF_6-PuF_6 mixtures were prepared on a given day and examined by thermal analysis the following day. Therefore the effect of alpha-destruction of hexafluoride molecules on composition was considered.

Both PuF_6 and UF_6 will be destroyed by the alpha radiation of plutonium in UF_6-PuF_6 mixtures. Lacking quantitative results on the rate of decomposition of solid UF_6 by alpha radiation, we assumed that in the solid state, UF_6 and PuF_6 are equally susceptible to destruction of alpha radiation.

The uranium compound formed by alpha decomposition of UF_6 solid is unknown. Shiflett et al.[31] were unable to identify the uranium compounds produced by the alpha decomposition of UF_6 vapor, but suggested that they were uranium fluorides of composition intermediate between UF_4 and UF_6. The product of alpha decomposition of liquid UF_6 is uranium pentafluoride.[32] Possibly the primary product of alpha decomposition of UF_6 vapor is a lower intermediate fluoride (U_2F_9 or U_4F_{17}) or UF_4, all of which compounds can react with UF_6 to produce a higher intermediate such as UF_5 (Ref. 33). Similarly, the primary product of alpha decomposition of UF_6 solid is probably UF_4 or a fluoride intermediate in composition between UF_4 and UF_6.

The products of alpha decomposition of UF_6 and PuF_6 can all undergo a recombination reaction with the fluorine to recreate the

hexafluorides. Also, Weinstock and Malm[4] demonstrated that PuF_6 will react with either UF_4 or the intermediate fluorides to produce UF_6 and PuF_4.

Considering all the above possibilities, the maximum change of composition of UF_6-PuF_6 mixtures caused by alpha destruction of the solids can probably be estimated by assuming that the primary product of alpha decomposition of UF_6 is UF_4, and that the UF_4 is completely fluorinated by PuF_6 as follows:

$$PuF_6 + UF_4 \rightarrow PuF_4 + UF_6. \tag{6}$$

This maximum effect is equivalent to the disappearance of 2% of the initial PuF_6 after a 1-day period. The mole fraction of UF_6 in a UF_6-PuF_6 mixture, corrected for the maximum effect of alpha decomposition, 1 day after preparation of the mixture was estimated by

$$N^r_{UF_6} = \frac{n_{UF_6}}{n_{UF_6} + 0.98\, n_{PuF_6}}, \tag{7}$$

where

n = initial moles of component,

and

$N^r_{UF_6}$ = mole fraction of UF_6 with maximum correction for radiation decomposition.

Values of the correction terms $(N^r_{UF_6} - X_{UF_6})$, which were added to the mole fraction $UF_6(X_{UF_6})$ calculated from the total moles of UF_6 and PuF_6, are listed in Table I.

2. Correction of Measured Temperatures

The iron-constantan thermocouple used to measure the temperature of the mixtures was calibrated against four other thermocouples previously calibrated directly against an NBS-standardized platinum resistance thermometer. As a result of the calibration procedures, a correction term of +0.3°C was added to the temperatures measured by the iron-constantan thermocouple.

APPENDIX B

Separation of UF_6-PuF_6 Mixtures by Fractional Crystallization; Calculation of Number of Equilibrium Crystallization Stages

Fractional crystallization is not under consideration as a means of separating UF_6-PuF_6 mixtures in a fluoride volatility flowsheet. The freezing-point diagram, however, can be used to estimate the separation of UF_6-PuF_6 mixtures by fractional crystallization. Since the condensed-phase equilibria involve a continuous series of solid solutions, the number of equilibrium stages needed to effect a given separation can be estimated by the graphical procedure of marking off steps on a diagram similar to the X-Y diagrams used in estimations on fractional distillation of binary liquid mixtures.[34] Figure 11 is a graph of mole fraction of UF_6 in the solid phase versus mole fraction of UF_6 in the liquid phase for solid-liquid equilibria in UF_6-PuF_6 mixtures. This graph can be used to estimate the number of equilibrium stages necessary to obtain a PuF_6 product of given purity from a given PuF_6-UF_6 feed mixture. Starting at a point corresponding to the feed composition on the operating line, the number of steps necessary to reach the composition of the desired product are marked off. The use of the 45° diagonal as the operating line corresponds to the condition of total reflux. The estimate of the number of equilibrium stages obtained from this procedure assumes perfect separation of crystals and mother liquor at each stage. In the terminology of Forsyth and Wood,[21]

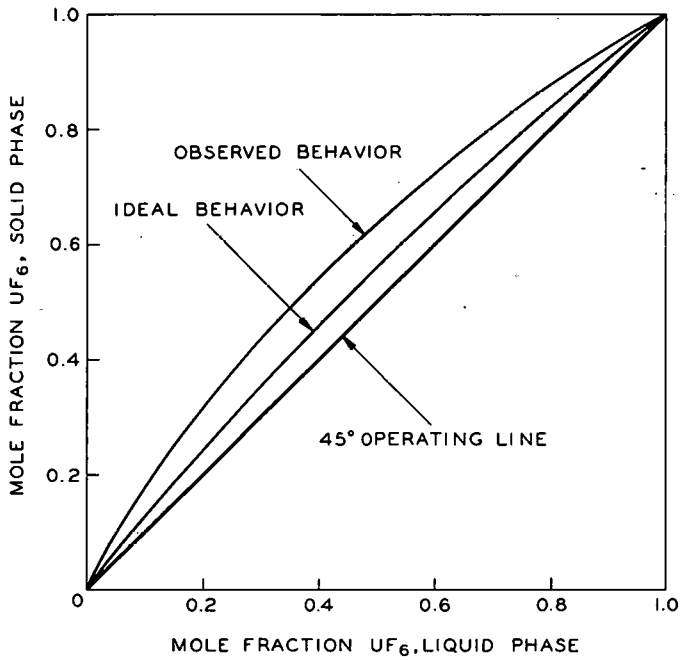

Fig. 11. X-Y Diagram, Solid-Liquid Phase Equilibria in the System UF_6-PuF_6

$$\text{Crystallization Efficiency} = \frac{\text{Difference in Composition between Solid and Liquid Phases}}{\text{Difference in Composition Theoretically Possible}} \times 100. \quad (8)$$

The estimates obtained from the stepping procedure assume a crystallization-stage efficiency of 100%. The number of stages for a given separation obtained by using Fig. 11, with the qualifications of total reflux

and the assumption of 100% crystallization efficiency, are minimum values. Real operation, employing product take-off, an operating line with a slope of less than 45° (less than total reflux), and stage efficiencies of less than 100%, would require a higher number of equilibrium stages for a given separation.

1. Number of Equilibrium Stages from Ideal Melting-point Diagram

For estimation of the number of stages for a separation in the case of ideal behavior, the values of mole fraction UF_6 in solid and liquid phases obtained from Eqs. 2 and 3 were plotted in Fig. 11. Since the separation factor,

$$\alpha \text{ crystallization} = \frac{\left(N_{UF_6}\right)_{solid} \times \left(N_{PuF_6}\right)_{liquid}}{\left(N_{UF_6}\right)_{liquid} \times \left(N_{PuF_6}\right)_{solid}} \qquad (9)$$

(where N = mole fraction), remains relatively constant over the entire range, the Fenske equation yields the number of equilibrium stages for a given separation as accurately as the graphic procedure. Using an average separation factor (α) of 1.30 and the Fenske equation in the form,[35]

$$n = \frac{\log \frac{\left(N_{UF_6}\right)_{feed}}{\left(N_{PuF_6}\right)_{feed}} - \log \frac{\left(N_{UF_6}\right)_{product}}{\left(N_{PuF_6}\right)_{product}}}{\log \alpha} - 1, \qquad (10)$$

the number of crystallization stages were calculated, which agreed with those obtained by the simple graphic stepping procedure on a 25-in. square graph. The equation indicates that 34 equilibrium stages will produce 99% PuF_6 from a feed containing 99% UF_6 if the UF_6-PuF_6 system were ideal.

2. Number of Equilibrium Stages from Observed Melting-point Diagram

If the observed solidus points do represent equilibrium conditions, they should be used to calculate the number of stages needed for separation. Smooth curves were drawn through the observed solidus points, and also through the observed liquidus points. The compositions of liquid and solid phases from these smooth curves were used to construct the curve in Fig. 11 for observed data. Since the separation factor calculated from the smoothed, observed data does not remain constant (varying from about 1.6 to about 2.6), results obtained by using the Fenske equation were not acceptable. The graphic procedure, used with the observed data, indicates that 15 equilibrium stages will produce 99% PuF_6 from a feed of 99% UF_6.

ACKNOWLEDGMENT

The authors wish to thank Mr. Irving E. Knudsen, for providing the sample of UF_6; Mr. James G. Riha, for contributing to the design of the sample tubes; Mr. George W. Redding and Mr. Milton Haas, for some of the instrumental operations; and Dr. John J. Barghusen, for a discussion of the use of the Fenske equation, and for his suggestions on improvement of the manuscript.

REFERENCES

1. Malecha, R. F., Smith, H. O., Schraidt, J. H., Natale, J. V., Ross, N. E., and Brown, H. L., Jr., "Low Cost Glove Boxes," *Proceedings of the Eighth Conference on Hot Laboratories and Equipment*, TID-7599, pp. 485-493 (1960).

2. Weinstock, B., Weaver, E. E., and Malm, J. G., *Vapor Pressures of NpF_6 and PuF_6; Thermodynamic Calculations with UF_6, NpF_6 and PuF_6*, J. Inorg. Nucl. Chem. 11, 104 (1959).

3. Kessie, R. W., *The Design and Construction of Thermal Flowmeters*, ANL-6531 (March 1962).

4. Weinstock, B., and Malm, J. G., *The Properties of Plutonium Hexafluoride*, J. Inorg. Nucl. Chem. 2, 380 (1956).

5. Findlay, A., *The Phase Rule and Its Applications*, pp. 474-476, Longmans, Green and Company, Inc., New York (1938); Republished by Dover Publications, New York.

6. Bullard, H. L., Ostroski, A. S., and Stringham, W. S., *Freezing Point Determinations of the Uranium Hexafluoride-Hydrogen Fluoride System*, GAT-213, Goodyear Atomic Corporation, Portsmouth, Ohio (Oct 1957).

7. Priest, H. F., and Priest, G. L., *The Depression of the Triple Point as a Means for Determining the Concentration of HF in Uranium Hexafluoride*, A-3627, Clinton Engineering Works, Carbide and Carbon Chemicals Corporation (April 1944).

8. Shenker, H., Lauritzen, J. I., Jr., Corruccini, R. J., and Lonberger, S. T., *Reference Tables for Thermocouples*, U. S. Department of Commerce, Natl. Bur. Standards Circular No. 561 (April 1955).

9. Wooley, J. C., and Smith, B. A., *Solid Solutions in $A^{III}B^{V}$ Compounds*, Proc. Phys. Soc. (London) 72, 214 (1958).

10. Hildebrand, J. H., and Scott, R. L., *The Solubility of Nonelectrolytes*, 3rd ed., pp. 300-319, Reinhold Publishing Corporation, New York (1950).

11. Reference 10, p. 129, Eq. 36.

12. Reference 10, p. 131.

13. Steindler, M. J., and Schablaske, R., "Lattice Constants for UF_6, NpF_6, and PuF_6," *Chemical Engineering Division Semiannual Report*, January-June 1964, ANL-6900, pp. 162-164 (Aug 1964).

14. Florin, A. E., Tannenbaum, I. R., and Lemons, J. F., *Preparation and Properties of Plutonium Hexafluoride and Identification of Plutonium (VI) Oxyfluoride*, J. Inorg. Nucl. Chem. 2, 368 (1956).

15. Lawson, A. W., *On Simple Binary Solid Solutions*, J. Chem. Phys. 15, 831 (1947).

16. Weinstock, B., *Rotation and Molecular Distortion in the Condensed Phases of Hexafluoride Molecules*, J. Phys. Chem. Solids 18, 86 (1961).

17. Blinc, R., Pirkmajer, E., Zupancic, I., and Rigny, P., *Relaxation Through Anisotropic Chemical Shift in Polycrystalline UF_6*, J. Chem. Phys. 43, 2927 (1965).

18. Rigny, P., *Anisotropy of the Fluorine Chemical Shift Tensor in UF_6*, Commissariat a l'Energie Atomique--France, CEA-R2827, Centre d'Etudes Nucleaires de Saclay (Aug 1964).

19. Seltz, H., *Thermodynamics of Solid Solutions. I. Perfect Solutions*, J. Am. Chem. Soc. 56, 307 (1934).

20. Biswas, A. K., and Bashforth, G. R., *The Physical Chemistry of Metallurgical Processes*, pp. 132-134, Chapman and Hall, Ltd., London (1962).

21. Forsyth, J. S., and Wood, J. T., *The Separation of Organic Mixtures by Crystallization from the Melt*, Trans. Inst. Chem. Engrs. (London) 33, 122 (1955).

22. Ricci, J. E., *Guide to the Phase Diagrams of the Fluoride Systems*, ORNL-2396, p. 5, Oak Ridge National Laboratory (Dec 1958).

23. Hume-Rothery, W., Christian, J. W., and Pearson, W. B., *Metallurgical Equilibrium Diagrams*, p. 153, The Institute of Physics, London (1952).

24. Wooley, J. C., and Lees, D. G., *Equilibrium Diagrams with InSb as One Component*, J. Less-Common Metals 1, 192 (1959).

25. Seltz, H., *Thermodynamics of Solid Solutions. II. Deviations from Raoult's Law*, J. Am. Chem. Soc. 57, 391 (1935).

26. Lewis, G. N., and Randall, M., *Thermodynamics*, 2nd ed., revised by Pitzer, K. S., and Brewer, L., pp. 416-417, McGraw-Hill Book Company, Inc., New York (1961).

27. Scatchard, G., and Hamer, W. J., *The Application of Equations for the Chemical Potentials to Equilibria Between Solid Solution and Liquid Solution*, J. Am. Chem. Soc. 57, 1809 (1935).

28. Wertz, R. J., and Hedge, W. D., *Density of Liquid Uranium Hexafluoride*, K-1466, Union Carbide Corporation Nuclear Division (Feb 1965).

29. Katz, J. J., and Rabinowitch, E., *The Chemistry of Uranium*, National Nuclear Energy Series, Manhattan Project Technical Section, Division VIII--Volume 5, p. 427, McGraw-Hill Book Company, Inc., New York (1951).

30. Wagner, R. P., Shinn, W. A., Fischer, J., and Steindler, M. J., *Laboratory Investigations in Support of Fluid-bed Fluoride Volatility Processes, Part VIII. The Decomposition of Gaseous Plutonium Hexafluoride by Alpha Radiation*, ANL-7013, p. 6 (May 1965).

31. Shiflett, C. H., Steidlitz, M. E., Rosen, F. D., and Davis, W., Jr., *The Chemical Effect of Alpha Particles on Uranium Hexafluoride*, J. Inorg. Nucl. Chem. 7, 210 (1958).

32. Steindler, M. J., Steidl, D. V., and Fischer, J., *Laboratory Investigations in Support of Fluid-bed Fluoride Volatility Processes, Part V. The Radiation Chemistry of Plutonium Hexafluoride*, ANL-6812, p. 4 (Dec 1963).

33. Agron, P. A., *Thermodynamics of Intermediate Uranium Fluorides from Measurements of the Disproportionation Pressures*, *Chemistry of Uranium, Collected Papers*, TID-5290, p. 610 (1958).

34. Findlay, R. A., and McKay, D. L., *Separation by Crystallization*, Chem. Eng. Progr. Symp. Ser., No. 25, 55, 163 (1959).

35. Perry, E. S., and Weissberger, A., (Eds.) *Technique of Organic Chemistry, Vol. IV Distillation*, 2nd Ed., p. 29, Interscience Publishers, New York (1965).